# CHAPTER 5

Investigations of the C-terminal domain on the refolding of OmpA tryptophan mutants using steady-state fluorescence and circular dichroism spectroscopy

*Acknowledgement:* Some experiments were done in collaboration with Dr. Judy E. Kim.

## 5.1 INTRODUCTION

*In vitro* refolding of integral membrane proteins has been reported for both α-helical (Huang et al., 1981; Paulsen et al., 1990) and β-barrel proteins (Dornmair et al., 1990; Eisele & Rosenbusch, 1990). These studies reconstituted the proteins in detergent micelles or mixed lipid/detergent micelles. Phospholipid vesicle membranes are considered to mimic the cell membrane geometry better than detergents. OmpA was the first report of a protein refolding directly into lipid vesicles from a denatured state. Compared to α-helical bundles, this β-barrel protein has a weaker propensity for aggregation in water due to its amphipathic β-sheet structure. The properties of OmpA make it an ideal model for investigation of refolding and membrane insertion (Surrey & Jahnig, 1992). Since this initital report, refolding of wild-type OmpA into lipid vesicles has been extensively studied (Dornmair et al., 1990; Surrey & Jahnig, 1992; Surrey & Jahnig, 1995). Since then, other β-barrel membrane proteins have also been studied, such as the porin OmpF, and have been shown to refold and insert from an unfolded state (Surrey et al., 1996).

As described in Chapter 2, OmpA contains two domains, a transmembrane N-terminal domain and a water-soluble, periplasmic C-terminal domain. The yield of refolding depends on various factors such as pH, lipid concentration and composition, temperature, and vesicle size (Surrey & Jahnig, 1995). At pH 10, the refolding yield of OmpA is nearly 100 % in pH 10, which agrees with the proteins being more soluble in water at highly basic (up to pH 10) or highly acidic conditions (below 2) (Surrey et al., 1996). At pH above 10, intramolecular charge may not allow refolding and insertion. At pH 7 in water, OmpA is only about 10 % soluble. At pH 7 and 1.5 mM DMPC lipid

concentration, which are the experimental conditions used throughout this thesis, the yield of refolding is ~60-70 %.

Folding of β-barrel membrane proteins is fundamentally distinct from folding of α-helical membrane proteins. In α-helical membrane proteins, hydrogen bonds are formed within individual helices whereas in β-barrel membrane proteins, they are formed between neighboring strands. The α-helix is capable of being independently stable, which allows insertion of individual helices into the membrane, followed by lateral assembly of the helices into bundles. In contrast, β-sheets cannot exist independently from the whole protein. The current OmpA folding model was originally developed by Surrey and Jahnig at the Max-Planck Insitute for Biology and then revised by the Tamm group at UVA (Surrey & Jahnig, 1995; Kleinschmidt et al., 1999; Kleinschmidt & Tamm, 2002). The major question regarding folding of β-barrel membrane proteins is whether folding and insertion are two separate processes or whether there are different folding intermediates, similar to the two-stage model of α-helical membrane proteins.

Early refolding kinetics revealed a partially folded intermediate that was detected by CD measurements and is thought to be the hydrophobically collapsed state detected in soluble proteins (Surrey & Jahnig, 1995). This state is thought to be a completely misfolded state similar to the state formed when OmpA is diluted directly into phosphate buffer. Upon folding into lipid vesicles, two slower processes were detected using CD and tryptophan fluorescence. The process with a 5 min half-time is believed to be the transition from the misfolded state to a more correctly folded state, corresponding to the molten globule of soluble proteins. The global structure of OmpA is formed during the molten globule state, but correct tertiary structure and details are still lacking. The other

process, with a 40 min half-time appears to correspond to the conversion from the molten globule state to the native state.

Results of the fast phase from gel insertion and fluorescence intensity increase were interpreted as OmpA initially adopting secondary structure while a small percentage inserts into the membrane. Therefore, at least three kinetic phases were observed in this early study. The transition from unfolded OmpA to an intermediate in water occurs within 1s. Association with membranes occurs in two phases with half-times of 5 min and 30 min, resulting in the native structure.

Addition of peptidyl-prolyl isomerase did not accelerate the folding kinetics and therefore ruled out proline isomerization as the slow step in OmpA folding. Refolding of the OmpA transmembrane region was studied and results were similar to those from the whole protein (Surrey & Jahnig, 1995; Surrey et al., 1996). As described in Chapter 3, the C-terminal tail is not required for oriented insertion of OmpA, suggesting that the orientation of OmpA appears to be related to the mechanism by which the protein inserts.

It is speculated that the adsorbed/partially folded state detected at 15 $^{o}$C with DMPC vesicles may be an intermediate in the folding process and that the state resembles a planar, amphipathic β-sheet flat on the surface of the vesicles with its hydrophobic side contacting the vesicle hydrophobic core. This state would then "roll" into the vesicle as the β-barrel is formed. As discussed in Chapter 3, two membrane bound forms of OmpA have been observed at temperatures above and below the gel-liquid transition temperature of DMPC. Consistent with reported literature, we also observed extensive β-sheet structure and a hydrophobic Trp environment for this adsorbed species (Chapter 3).

The intermediate in water is analogous to the hydrophobic collapse state followed by the molten globule in soluble proteins, which is partially folded but lacking detailed structural elements. OmpA in this state may look like an "inside-out" version of the native structure.

As described in Chapter 4, the two membrane bound forms of OmpA were further characterized by FTIR and fluorescence spectroscopy with heavy atom quenching by membrane bound bromines. It was concluded that the membrane bound form is actually partially inserted and that reorientation of β-sheets take place when OmpA is inserted in the bilayer (Rodionova et al., 1995). However, it was not clear from Rodionora's work whether OmpA in the adsorbed state was induced from initially cold vesicles or from warm vesicles and then incubated at low temperatures. Also, the brominated lipids could have introduced local defects into the SUVs that allowed OmpA to partially insert at low temperatures. It is possible that instead of studying the adsorbed species, the authors actually studied an inserted intermediate on its way to the native structure.

Further studies by the Tamm group at UVA used DOPC vesicles, which have a gel-liquid-crystalline transition temperature of -18 $^{o}$C, allowing them to identify and trap intermediates stabilized in a wide range of temperatures from 2 $^{o}$C to 40 $^{o}$C. Specifically, two membrane bound intermediates were identified. Refolding as a function of temperature was monitored using SDS-PAGE, trypsin proteolysis, and Trp fluorescence. The first step observed was attributed to the fast hydrophobic collapse of OmpA in water. This is followed by two membrane bound intermediates, one that quickly associates to the vesicles ($1/k_1$ = 6 min) and another that inserts into the bilayer ($1/k_2$ = minute to hour timescale depending on temperature). Finally, folding to the native structure occurs in a

rate limiting step ($1/k_3$ = 2 hours at high temperatures). Temperature jump experiments also show that the low temperature species may convert with similar kinetics to the high temperature species. The results were analyzed using first-order kinetics since they use a large molar excess of lipids and because OmpA self-association is assumed to be negligible. The rate constant $k_1$ is temperature independent while $k_2$ and $k_3$ are highly temperature dependent. During the last step of folding, the formation of a smaller compact structure is seen by gel, and trypsin digestion suggests the insertion of this species (Kleinschmidt & Tamm, 1996).

Further insight into the mechanism was provided by time-resolved distance determination by Trp fluorescence quenching (TDFQ), which revealed the average movement of the five Trps during OmpA folding into brominated lipids (Kleinschmidt & Tamm, 1999). This technique was used to monitor Trp movement at temperatures from 2 $^{o}$C to 40 $^{o}$C. Quenching of the Trp fluorescence was observed even at the start of the refolding experiments, verifying that OmpA adsorbs to the bilayer surface within the mixing deadtime of 1-2 min. This technique revealed three membrane bound intermediates during the folding process. TDFQ was further utilized to study single Trp mutants during the course of folding, measuring the movement of specific regions of the protein. Results show that W7 remains on the exterior of the vesicles and never crosses the bilayer center while the other 4 Trp residues translocate across the bilayer at similar rates. Since these 4 Trps are located on 4 different outer loops of the 4 β-hairpins, it was concluded that OmpA inserts and folds into lipid bilayers by a concerted mechanism and that the 4 β-hairpins traverse the bilayer synchronously (Kleinschmidt et al., 1999).

Additional studies using CD to probe secondary structure formation and gel-shift assays to probe tertiary structure formation led to the conclusion that secondary and tertiary structures are formed synchronously. The authors suggest that β-sheet formation is correlated to closure of the β-barrel, and that these two processes are coupled to the insertion process (Kleinschmidt & Tamm, 2002).

Collective experiments from Surrey and Jahnig and the Tamm group greatly contributed to the current folding model of OmpA (Figure 5.1). The protein first undergoes hydrophobic collapse during its initial contact with water. In the presence of lipid vesicles or detergent micelles, adsorption to the bilayer is favored over aggregation in solution and rapidly occurs within several minutes to produce the first intermediate ($I_1$). It was originally thought that $I_1$ contains folded β-hairpins (Kleinschmidt & Tamm, 1999) but the model was later revised to one where $I_1$ has not yet been fully characterized (Kleinschmidt & Tamm, 2002). OmpA penetrates the membrane as the β-barrel is formed to produce the second membrane bound intermediate ($I_2$), described as a molten disk. In $I_2$ the Trp residues (excluding W7) and hairpins are located deeper in the membrane about ~10 Å from the bilayer center. Distance calculations indicate that the two central hairpins containing W102 and W57 reach this intermediate ($I_2$) faster than the peripheral hairpins. These hairpin Trps then move to the center of the bilayer, resulting in an intermediate ($I_3$) analogous to the molten globule in soluble protein folding. This version of the molten globule would be inside-out with the hydrophobic residues on the protein exterior interacting with the membrane and the hydrophilic residues located on the protein interior. Some β-hairpin hydrogen bonds are formed at this stage. The native structure is formed once the hairpins are translocated, placing the 4 hairpin Trps ~ 10 Å

from the bilayer center on the interior side of the vesicles. This type of synchronous folding, or some form of it, may also be relevant to ion channels, which are helical bundles composed of internal polar side chains.

Our overall goal is to contribute further insight into the molecular mechanism of OmpA folding. The role of the C-terminal in the folding has not previously been addressed in great detail. While it was reported that the kinetics of trypsin-truncated wt-OmpA are similar to full-length wt-OmpA, no data were shown in the literature (Surrey & Jahnig, 1995). Also since the kinetics were an average of all 5 Trps, it did not dissect any underlying kinetic differences among the Trp locations. The goal of this Chapter is to determine what role the C-terminal domain plays in the refolding kinetics of site-specific regions of OmpA. We use steady-state fluorescence (SSFl) and circular dichroism (CD) spectroscopy to monitor Trp environments and the overall formation of secondary structure in both full-length and truncated Trp mutants.

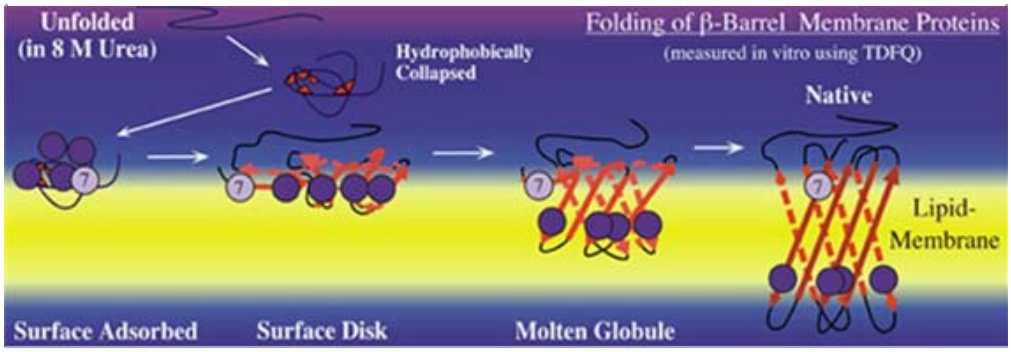


**Location of Tryptophan in Folding Intermediates Identified by TDFQ**

| Tryptophan | Distance from Center I | II | III | N |
|---|---|---|---|---|
| ⑦ | 14-16 Å | 10 Å | 10 Å | 10 Å |
| 15, 57, 102, 143 | | 10 Å | 0-5 Å | 10 Å |

**Figure 5.1.** Schematic of the current model of OmpA folding into the lipid bilayer. The chart indicates the average distances of the Trp residues from the center of the bilayer for each intermediate and the native structure. Adapted from (Kleinschmidt, 2003).

## 5.2 EXPERIMENTALS

Refolding kinetics of the tryptophan mutants were recorded using circular dichroism (CD) and steady-state fluorescence (SSFl) spectroscopy, which are described in the Materials and Methods section in Chapter 3. One additional difference in SSFl measurements is that samples containing deoxygenated background solutions of only urea, buffer, micelles, or vesicles were recorded prior to protein injection. In order to collect complete fluorescence scans every minute, a 3 nm/step and 0.1 s integration time were used. For CD measurements, background samples were not deoxygenated. Scans were acquired using 1 nm/step, 3 s integration. Protein samples of ~3-5 μM were injected manually using a syringe for CD spectra or using a syringe pump for SSFl spectra. Scans were programmed to collect at set time intervals for a duration of 2 hours at 30 $^{o}$C or 1 hour at 15 $^{o}$C. UV-visible absorption spectra were measured for the background solution and following 1-2 measurements for the protein samples, which were then placed back into the cuvette holder for the remainder of the measurements. For 15 $^{o}$C refolding of OmpA onto DMPC vesicles, the intensity at 330 nm was also observed over a period of 1 hour by exciting the sample at 290 nm and monitoring the emission at this single 330 nm wavelength.

For SSFl scans over the folding course, data were analyzed by subtracting background-only spectra from all protein spectra. The values at 330 nm from all scans were plotted against time to track the refolding kinetics. Upon folding, two processes occur as the Trps are placed in a more hydrophobic environment: $\lambda_{max}$ blue-shifts and quantum yield increases. To determine which of these two processes occurs faster, blue-

shifting was tracked by plotting $\lambda_{max}$ vs time and quantum yield increase was tracked by plotting either integrated intensity vs time or maximum intensity vs time.

## 5.3 RESULTS AND DISCUSSION

### *Refolding kinetics monitored by steady-state fluorescence: 30 $^{o}C$*

The refolding kinetics of full-length and truncated Trp mutants have been investigated in DMPC vesicles using Trp fluorescence. Changes in Trp fluorescence correspond to the binding and insertion of Trp into the hydrophobic bilayer. As described in section 5.1, previous studies on the refolding of full-length single Trp mutants have been performed using DOPC vesicles in a temperature range of 2 $^{o}$C to 40 $^{o}$C (Kleinschmidt et al., 1999). Removal of the C-terminal domain has been shown to have no affect on the ability of the protein to refold and orient itself into the membrane (Surrey & Jahnig, 1992). However, studies on the refolding kinetics of single Trp mutants without the C-terminal tail have not been reported. We chose to study refolding in DMPC since classic studies by Surrey and Jahnig were done with this lipid and we did not see significant folding in DOPC vesicles compared to DMPC vescicles. The following discusses our investigations into whether the C-terminal tail affects the refolding rate of specific Trp sites of OmpA.

In phosphate buffer, the protein displays an emission max of ~346 nm and does not show any systematic shifts over a 1 hr period (Figure 5.2). This shows that despite the residual structure in water as indicated by CD (Figure 3.12), initial dilution into vesicle solution results in a relatively polar Trp environment.

Immediately following protein injection to initiate folding into DMPC vesicles at 30 $^{o}$C, the fluorescence spectra of all mutants during the 120 minute folding reaction generally show a blue-shift in emission maximum and an increase in quantum yield (QY) (Figures 5.3 and 5.4). Analyses of these two processes reveal that the blue-shift and quantum yield increases exhibit different kinetics and therefore are not coupled. When the emission max ($\lambda_{max}$) is plotted along with integrated intensity ($I_{int}$), the blue-shift is observed to be faster than the rise in intensity for all Trp mutants (Figures 5.5-5.10). Blue-shift in $\lambda_{max}$ is essentially complete in about 20 minutes while the quantum yield continues to rise for ~2 hours. The blue-shift process corresponds to the Trps being placed in a more hydrophobic environment, which we interpreted as the protein undergoing the intial hydrophobic collapse. The quantum yield continues to rise until the end of folding, which we interpreted as expulsion of water from the protein as tertiary structure is formed. This interpretation is supported by the observation that lifetime of excited Trp in $D_20$ is longer than the lifetime in $H_20$ (Gudgin et al., 1983). Therefore, lifetimes are quenched in the presence of water. It is reasonable that we observe an increase in quantum yield since our measured Trp lifetimes are longer in folded protein than those of unfolded protein (Table 3.7). It is established that an increase in quantum yield ($\Phi$) is directly correlated with an increase in the excited-state lifetime ($\tau$) since they are related by $\Phi = k_r/k_{obs}$ where $k_r$ is the radiative rate constant and $k_{obs} = 1/\tau$ (Lakowicz, 1999).

Although these two processes, blue-shift and QY increase, were previously recognized in wt-OmpA to follow different kinetics (Kleinschmidt & Tamm, 1996), spectra showing these differences have not yet been reported and it is interesting to see

the changes evolving over time. When the emission max and integrated intensity plots for each mutant are overlayed, we see that all mutants have similar rates of blue-shift and quantum yield increase (Figure 5.5). Interestingly, W102 appears to be slightly faster than other mutants for both processes. The integrated intensity follows the same trends in kinetics between full-length and truncated mutants.

The intensity at 330 nm was used as a marker from each SSFl scan to follow the folding kinetics over time (Figure 5.11). The kinetics appear to be biphasic, consistent with published results for wild-type OmpA in DMPC vesicles (Surrey & Jahnig, 1995). A comparison of folding kinetics between the 10 mutants shows that there are modest kinetic differences between the various tryptophan positions. This small variance in kinetics at the various sites is consistent with the synchronous translocation of β-hairpins in the current OmpA folding model developed by the Tamm laboratory (Kleinschmidt et al., 1999).

Despite the modest variations in kinetics, general trends were observed in the folding plots for the full-length mutants. The kinetics appear to be reproducible for most mutants, although certain mutants (W143, W57t) show variable kinetics, possibly due to slight variations in vesicle size and concentration between data sets measured on different days. In the full-length data set (Figure 5.11), W102 appears to be in a more hydrophobic environment and inserts into its native environment faster than the other Trps. The rapid change in the W102 environment is consistent with reported results that W102 is one of the two fastest Trps to reach the 10 Å distance from the bilayer center (Kleinschmidt et al., 1999). The W102 insertion is followed by W15, W57, and W143 respectively. In contrast, W7 appears to be the slowest to reach its native environment. This seems

reasonable since the W15, 57, 143, and W102 must insert into the membrane and fold before the complete barrel is formed. It was also observed by Tamm and co-workers that W7 fluorescence kinetics in DOPC at 40 $^{o}$C contains a slow phase not observed in the other Trp mutants (Kleinschmidt et al., 1999). Kinetics differences between our experiments and those of Tamm's are probably due to the use of different lipid vesicles and temperatures.

The clear differences in fluorescence kinetics are not observed in the truncated proteins (Figure 5.12), although W7t kinetics still appears to be slightly slower than the other Trps. The lack of clear differences suggests an interaction of the large C-terminal domain with the N-terminus in the full-length protein is responsible for the differences in rates of folding and insertion. Removal of the C-terminus prevents this interaction, eliminating the differences that were seen with full-length mutants. When the kinetics between full-length and truncated mutants at each Trp position are overlaid, we see the kinetics are not exactly the same for certain mutants. W7t and W57t appear to be slightly faster than their full-length counterparts while W102t appears to be slightly slower than the full-length protein. W15 and W15t, as well as W143 and W143t, have similar fluorescence kinetics. Others have not seen kinetic differences between full-length and truncated OmpA, perhaps due to inadvertently canceling out differences by signal averaging of the 5 Trps.

The slow fluorescence kinetics of W7 suggest that this environment is the last to arrange into the native state after most of the β-structure has already formed. W7 may also be slow due to its possible greater interaction with the C-terminal domain. In Chapter 3, we observed that the anisotropy of W7 is low and decays to a lower value

faster than the other Trp residues. In the truncated form, W7t no longer has as large an interaction with the C-terminal domain and is allowed to reach its native environment faster than its full-length counterpart, but still slower than the other Trps. Fluorescence quenching of W7 by brominated lipids (Chapter 4) also indicates that W7 is the closest Trp residue to the bilayer center. The slow expulsion of water from this relatively deep site is likely slower than at more exposed sites and could also account for the slower fluorescence kinetics.

Another scenario is that mutation of the other four Trp to Phe could have affected the translocation rate across the bilayer. It is known that membrane proteins contain more Trp than soluble proteins and that Trp may possibly help translocate membrane proteins into the bilayer during folding (Schiffer et al., 1992). The overall loss of 4 Trp residues in the β-hairpins may have affected the rate of translocation across the membrane. If folding is greatly affected by the loss of these hairpin Trp, we would observe slower formation of secondary structure. However, this is not believed to be true since our CD kinetics do not show a drastic difference in the overall β-sheet formation for W7 compared to the other Trp (Figure 5.20 and 5.21).

In summary, the fluorescence kinetics suggest that the C-terminal tail may slightly affect the refolding rates through the increase or decrease of the folding rate of certain sites. Site specific kinetics allowed us to detect these subtleties that were otherwise not observed using the truncated wt-OmpA.

***Refolding kinetics monitored by steady-state fluorescence: 15 $^{o}$C***

At 15 $^{o}$C, the DMPC vesicles are in a gel-like state, preventing the protein from folding into the bilayer. Instead, OmpA has been shown to adsorb to the surface of the

vesicles (Surrey & Jahnig, 1992; Surrey & Jahnig, 1995). We investigated the refolding kinetics of the mutants at 15 $^{o}$C. Results show that after protein injection, an increase in fluorescence intensity is observed within a few minutes and the fluorescence values do not change drastically over a 1 hr period unlike those at 30 $^{o}$C (Figures 5.14-5.16). SSFl scans show that almost immediately (within a few minutes at most), the spectra are blue-shifted and remain approximately the same over a 1 hr period. Measurement of the intensity at 330 nm for all mutants also showed that the value remains steady (Figure 5.17). The Trps are immediately placed in a hydrophobic environment and little structural changes are observed while in the adsorbed state, which is confirmed by CD measurements at 15 $^{o}$C (described below).

***Refolding kinetics monitored by circular dichroism: 30 $^{o}$C and 15 $^{o}$C***

CD spectra recorded at 30 $^{o}$C over a period of 2 hours after protein injection into vesicles are shown in Figures 5.18 and 5.19 (left side). Initially, the spectra show no β-sheet signal but look similar to the CD of mutants in buffer (Figure 3.3), which is a reasonable comparison since this is the environment first encountered by the protein when added to a vesicle solution. Structural conformations begin to form as indicated by the appearance of β-sheet signal, ~20-30 min into folding, and continue as the protein evolves to the native state. Scans were collected every few minutes however some were omitted in the figures for clarity. Spectra showing the evolution of β-sheet signal during folding as shown here have not yet been reported.

Ellipiticity values at 206 nm were plotted as a function of time to show the general kinetics of β-sheet formation (Figure 5.20) for both the full-length and truncated Trp mutants. The overall kinetics are similar within the full-length and the truncated

mutants. It should be noted that CD measures the global rearrangements rather than site-specific changes. Kinetic rates were not obtained from these plots since the signal to noise ratio is too low. Noisy scans were a result of rapidly integrated scans in order to acquire time points every few minutes.

CD spectra recorded at 15 $^{o}$C during the 1 hour period after protein injection into vesicles are shown in Figures 5.18-5.19 (right side). They are consistent with previous reports that the low temperature adsorbed species adopts a β-sheet structure (Surrey & Jahnig, 1992). Both the full-length and truncated mutants show that almost immediately, the adsorbed protein adopts a highly β-sheet structure, and essentially no conformational changes are observed over a 1 hour period. Note that the full-length protein requires slightly longer times compared with the truncated protein to develop the β-sheet signal. This is probably due to the higher amount of urea in the final solution since full-length protein stocks were not as concentrated. The immediate development of secondary structure confirms results from SSFl scans where the Trp environment becomes hydrophobic almost immediately. The proteins adopt an ordered β-sheet structure, placing the tryptophans in a hydrophobic environment. This β-sheet structure is most likely misfolded and not similar to the native protein since a hydrophobic environment (micelles or vesicles) is required to surround the native structure, allowing the hydrophobic residues to point outward.

It would be interesting to further characterize the structure of this adsorbed species. Does it have any components of the native like structure? There are 4 tryptophan residues (7, 15, 57, 143) that face the lipid bilayer environment in the native structure. It would be interesting to determine where these tryptophan residues are in

relation to the bilayer in the adsorbed species. They may all somehow be pushed against the surface of the bilayer or they may be buried inside the protein structure, which is presumably misfolded. Attempts to characterize this intermediate in detail by Rodionova and co-workers (1995) concluded that this species is partially inserted. However, as discussed in Chapter 4, it is not clear whether the species they studied were actually the adsorbed species or whether they were the second intermediate ($I_2$) in the folding process that is inserted due to warm vesicles or from defects due to the longer brominated lipids.

It is possible that the low and high temperature species exist in equilibrium at the start of folding. By shifting the temperature either higher or lower than the gel-liquid temperature, the equilibrium may be shifted in favor of one species over the other. At 30 $^{o}$C, an unstructured intermediate may be favored while at 15 $^{o}$C, a highly ordered structure with β-sheet content is observed. Therefore, it is not conclusively known whether the adsorbed species, which has not been fully characterized, is an intermediate in the folding process. In Chapter 6, FET kinetics are used to obtain the distance between W7 and the end of the barrel in this low temperature species, and the idea that this is not a true intermediate in the folding pathway will be discussed.

This investigation provides evidence for fast β-sheet formation upon protein dilution into vesicles at low temperatures using CD, but β-sheet formation does not happen until about ~30-40 min into the folding reaction for high temperatures. In the folding model, it was thought that $I_1$ contains secondary structure at the surface of the bilayer (Rodionova et al., 1995; Kleinschmidt et al., 1999). Later the authors revised the model, stating that the adsorbed species is actually made of incorrectly folded protein and that the structured parts are on the interior of the hydrophobic core (Kleinschmidt &

Tamm, 2002). The results described here support that the intermediate is some unstructured or misfolded state.

The adsorbed species at low temperatures may possibly be viewed as a connected series of independent β-hairpins in a star-like arrangement. However the reason for immediate β-sheet formation during the adsorbed state is not known. Is this star-like species actually formed in the process of OmpA refolding during optimal folding conditions, or is this species a trapped misfolded state that only occurs at low temperatures? It is possible that at higher temperatures, the energy is provided to overcome the barrier from the misfolded species to the native species.

It is unlikely that correct or native secondary structure is formed at the start of folding during adsorption. This differs from the two-stage model for α-helical membrane proteins where secondary structure is formed in stage I, followed by tertiary structure formation in stage II. The fundamental difference between α-helical bundles and β-barrels lies in the hydrogen bonding networks in the two motifs. It is energetically unfavorable to transfer a hydrogen bond to a more hydrophobic lipid environment (White & Wimley, 1999).

## 5.4 CONCLUSIONS

The goal of this Chapter is to determine whether the C-terminal domain plays a role in the refolding mechanism of OmpA. Steady-state fluorescence spectroscopy was employed to study the refolding of site-specific regions using tryptophan fluorescence as a reporter of binding and insertion. We used circular dichroism (CD) spectroscopy to determine the overall β-sheet formation of the mutants during the refolding time. From our kinetic scans, we observe that all Trp mutants undergo a hydrophobic collapse that is complete within 20 minutes. Insertion and expulsion of water are likely to take place as the quantum yield continues to rise until the end of folding. CD scans taken over the refolding period show that β-sheet signal appears in about 20-30 minutes, well after blue-shift is complete. This is consistent with the OmpA folding model where the protein first undergoes hydrophobic collapse, followed by insertion and formation of hydrogen bonds and finally the formation of the final tertiary structure.

At low temperatures, when the vesicles are in a gel state, OmpA quickly adsorbs to the surface of the vesicle and the tryptophans are immediately placed into a hydrophobic environment. At the same time the protein immediately forms β-sheet structure and no further secondary structural changes are observed. This adsorbed species is not likely an intermediate in the folding pathway since β-sheet signal is not initially observed in the refolding process at high temperatures. By monitoring the fluorescence intensity at 330 nm, we demonstrated that the C-terminal domain appears to play some kind of role in the refolding of the tryptophan residues. Full-length W102 inserts and forms the native environment the fastest, while W7 is the slowest. Removal of the C-terminal domain eliminates the differences seen in the full-length kinetics.

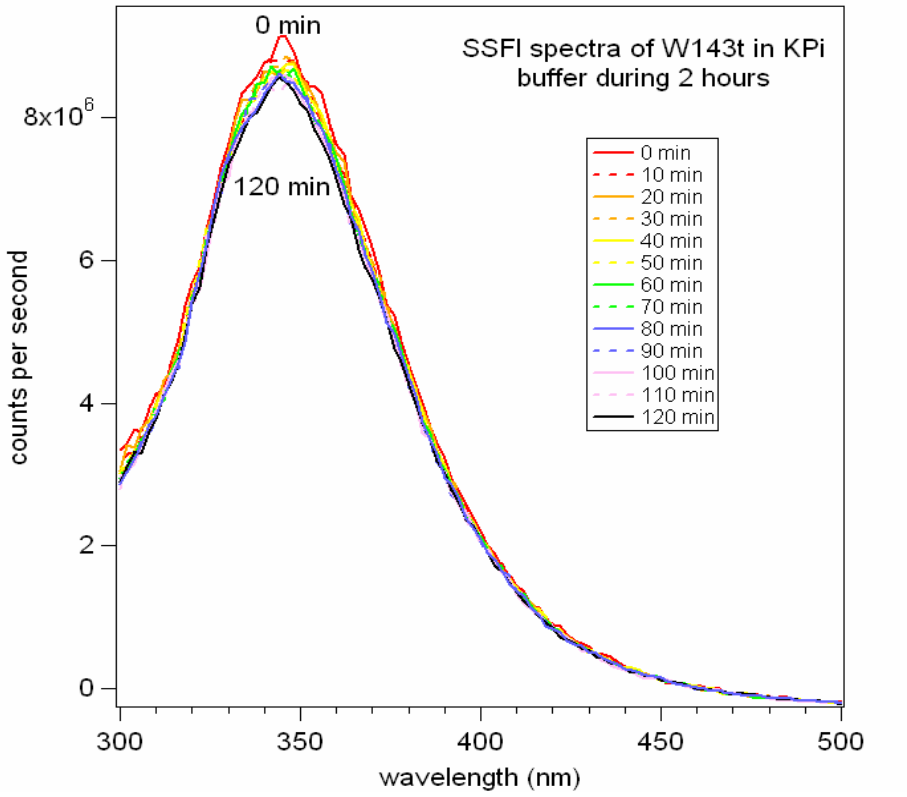


**Figure 5.2.** Fluorescence spectra of W143t immediately following greater than 120 fold dilution of 8 M urea into phosphate buffer (KPi). During the 120 minute reaction, the spectra showed no systematic shifts.

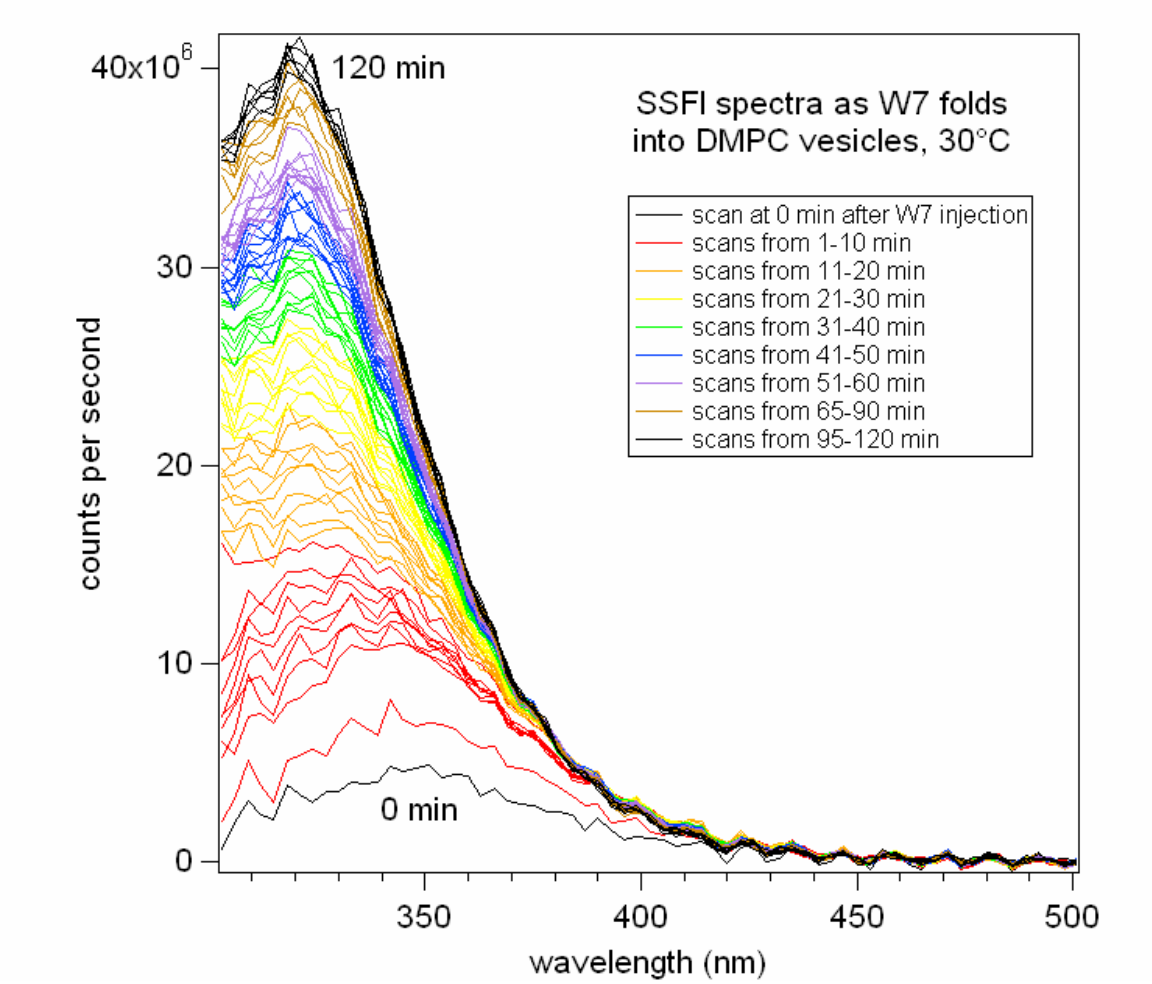


**Figure 5.3.** Fluorescence spectra of full-length W7 mutants immediately following protein injection to initiate folding into DMPC vesicles at 30 °C. During the 120 minute folding reaction, general changes in the spectra are observed in the form of a blue-shift in emission maximum and an increase in quantum yield.

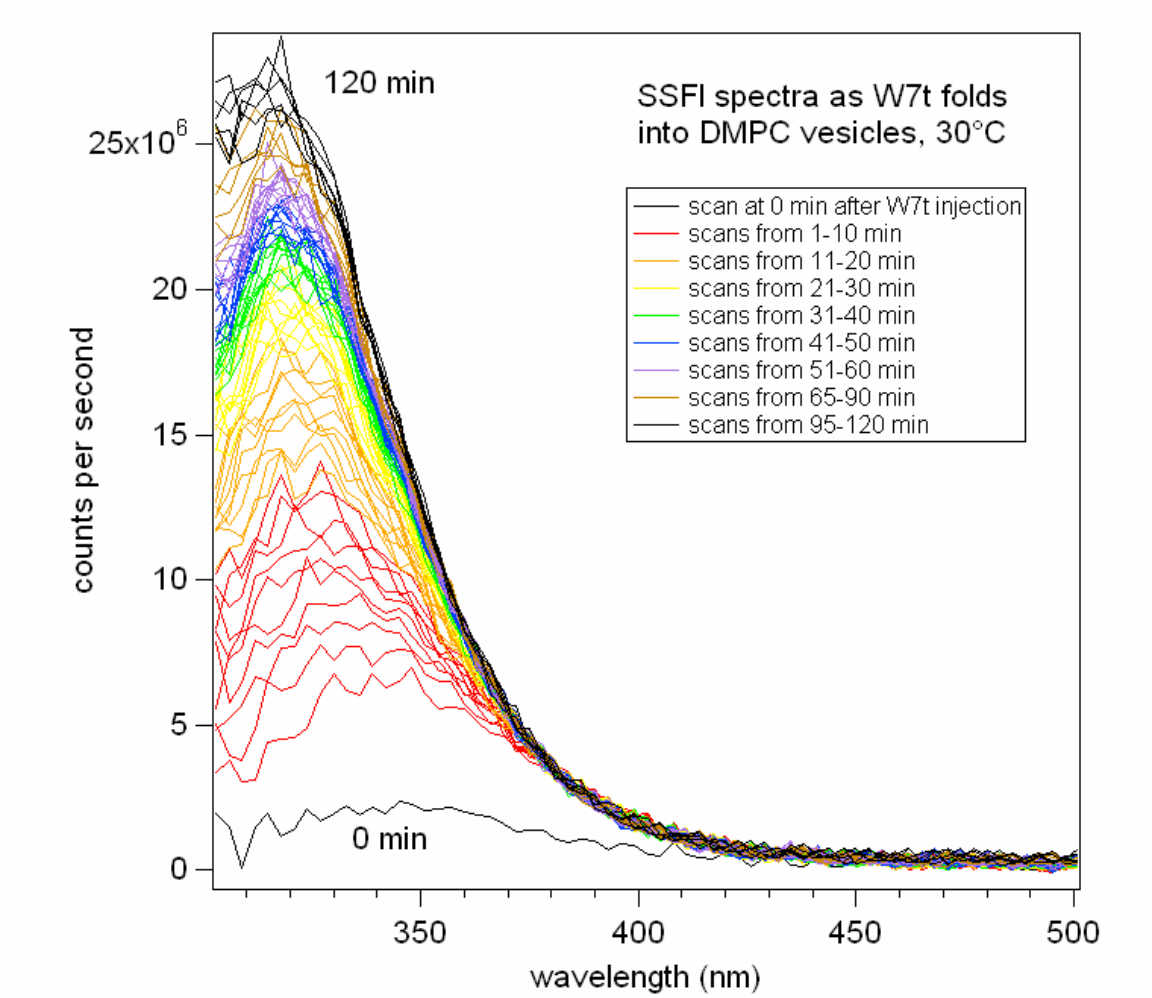


**Figure 5.4.** Fluorescence spectra of W7t immediately following protein injection to initiate folding into DMPC vesicles at 30 $^{o}$C. During the 120 minute folding reaction, general changes in the spectra are observed in the form of a blue-shift in emission maximum and an increase in quantum yield.

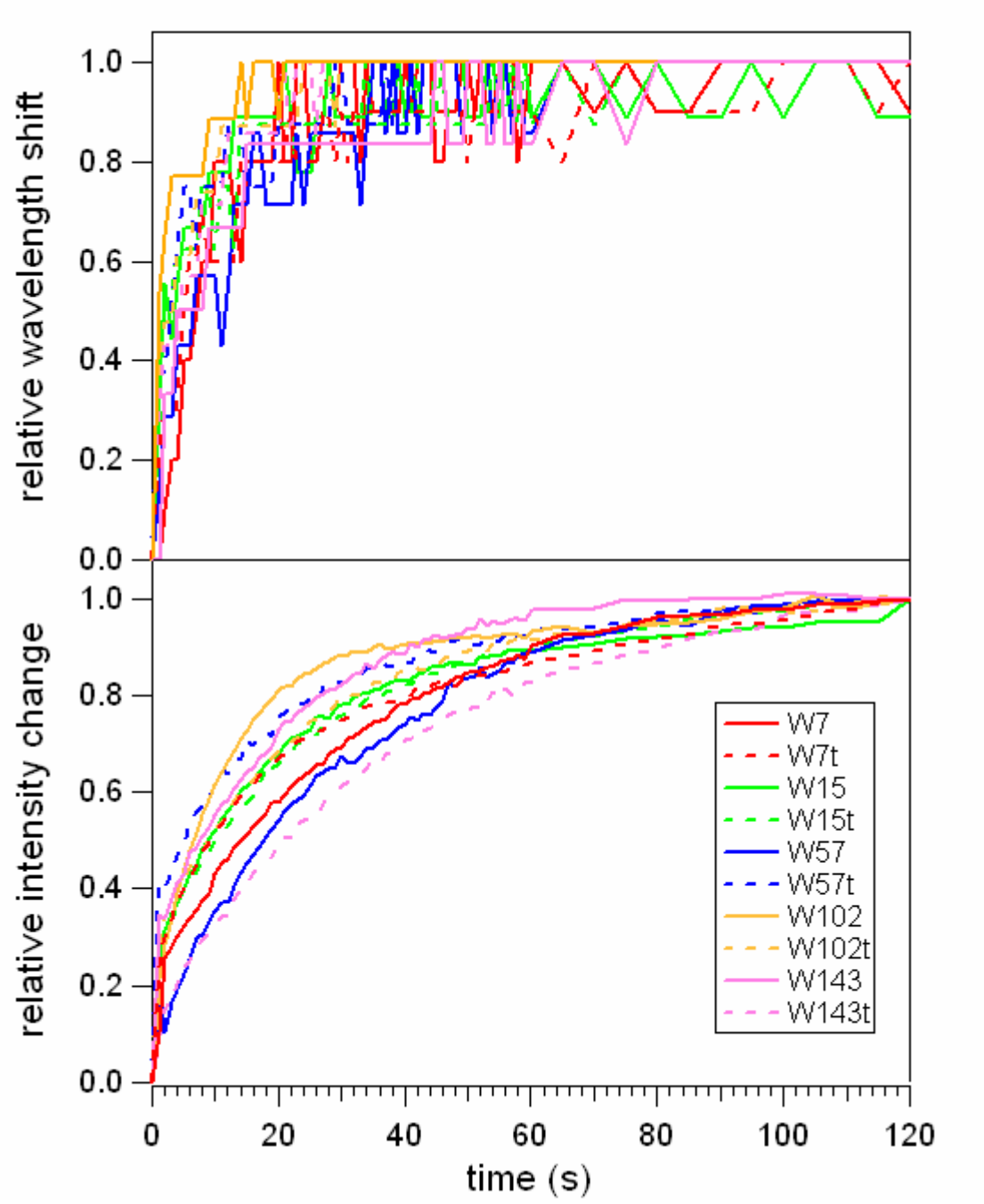


**Figure 5.5.** Relative changes in emission maxima (top) and emission intensity (bottom) as a function of folding time. A value of "1" indicates the final emission maximum or intensity at t = 120 minutes.

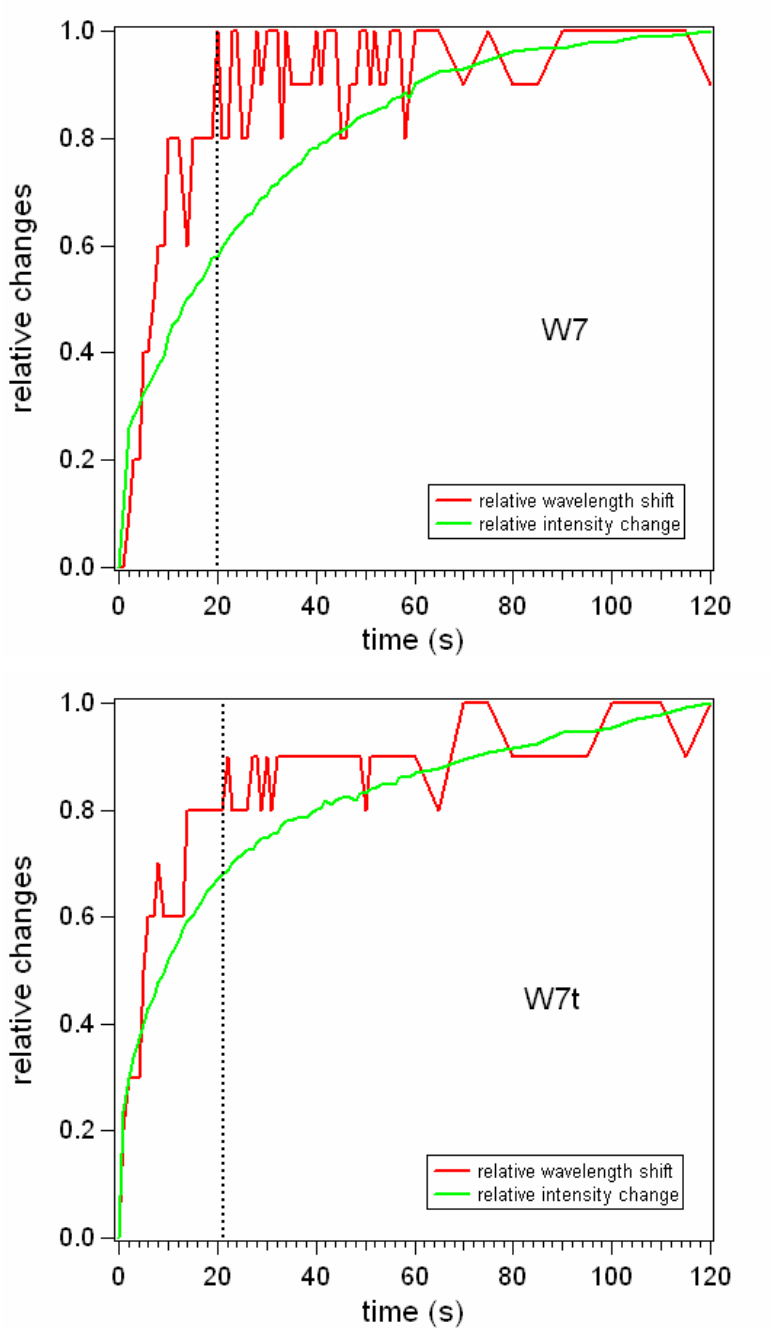


**Figure 5.6.** Comparison of the rate of blue-shifting and quantum yield increase for W7 and W7t. Dotted line indicates the approximate time when blue-shift is complete while quantum yield continues to increase.

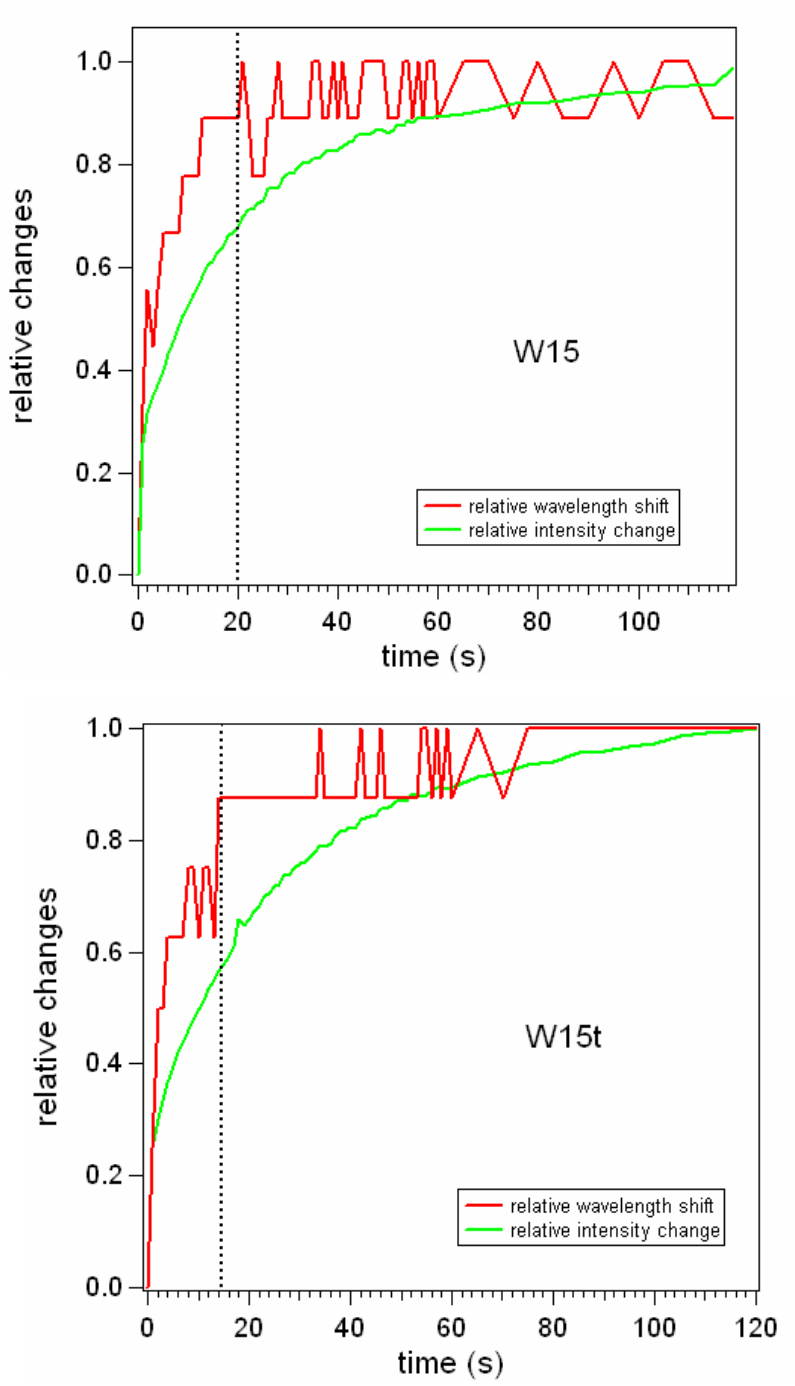


**Figure 5.7.** Comparison of the rate of blue-shifting and quantum yield increase for W15 and W15t. Dotted line indicates the approximate time when blue-shift is complete while quantum yield continues to increase.

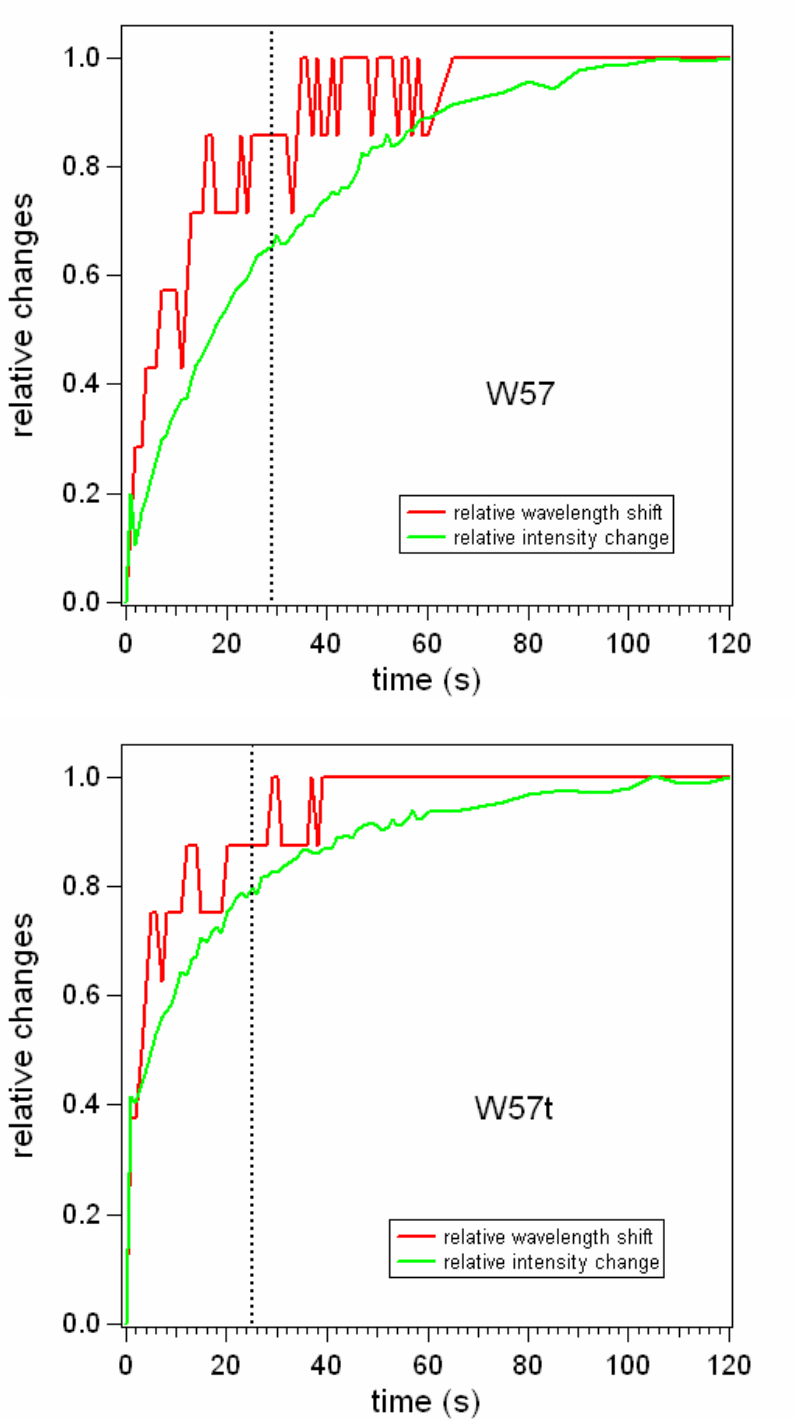


**Figure 5.8.** Comparison of the rate of blue-shifting and quantum yield increase for W57 and W57t. Dotted line indicates the approximate time when blue-shift is complete while quantum yield continues to increase.

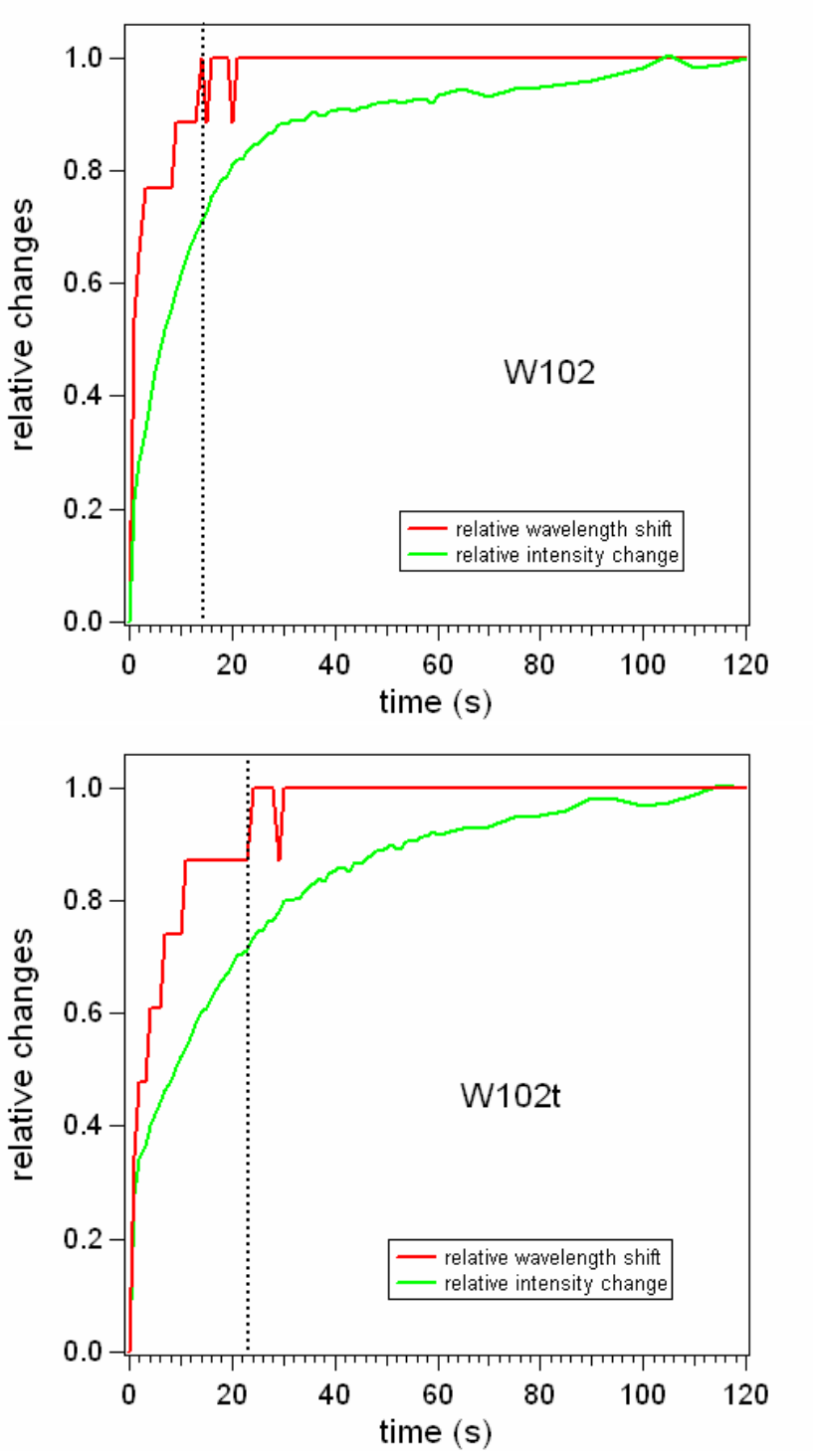


**Figure 5.9.** Comparison of the rate of blue-shifting and quantum yield increase for W102 and W102t. Dotted line indicates the approximate time when blue-shift is complete while quantum yield continues to increase.

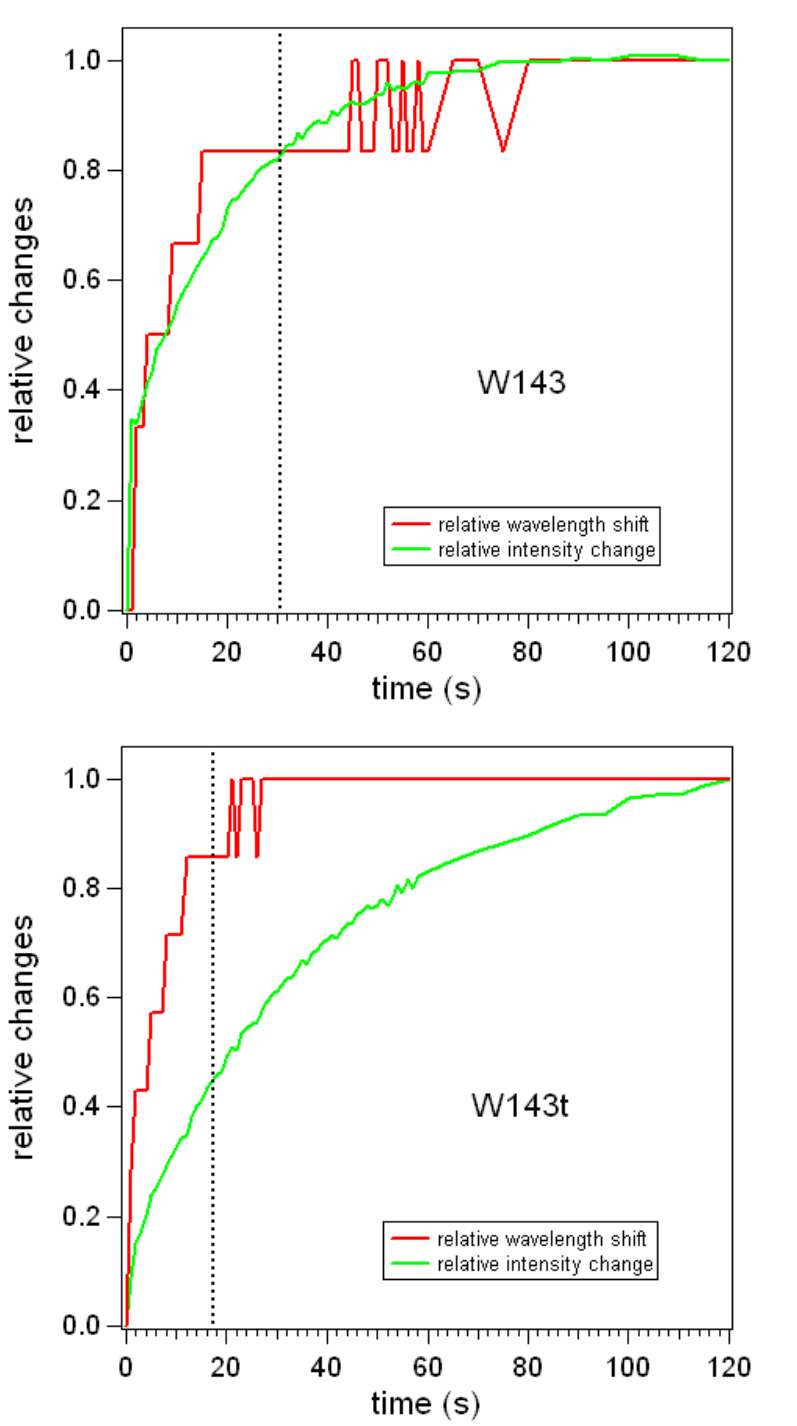


**Figure 5.10.** Comparison of the rate of blue-shifting and quantum yield increase for W143 and W143t. Dotted line indicates the approximate time when blue-shift is complete while quantum yield continues to increase.

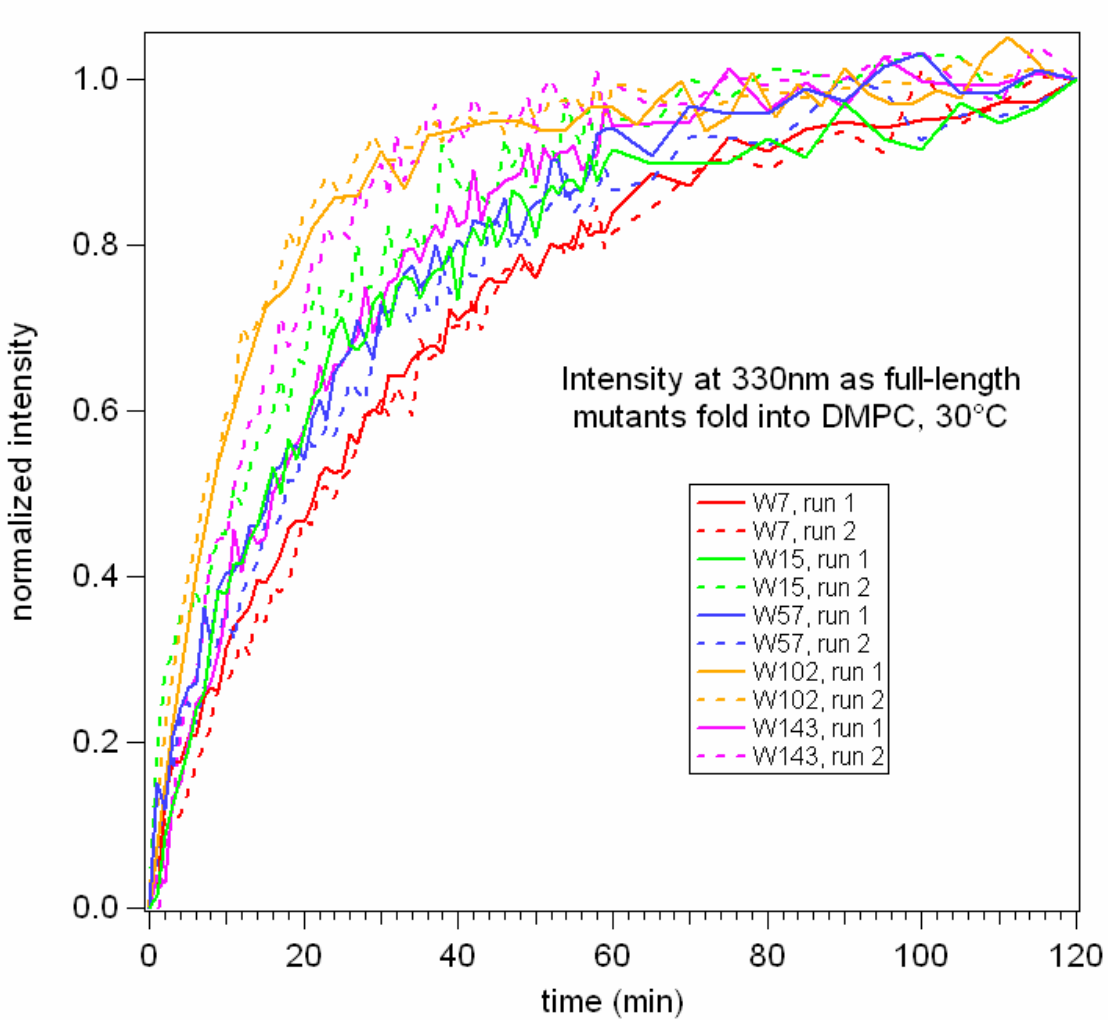


**Figure 5.11.** Fluorescence intensity of Trp mutants monitored at 330 nm immediately following initiation of folding reaction in DMPC for full-length mutants. Kinetic traces were normalized to have equivalent maximum emission intensities at 120 minutes.

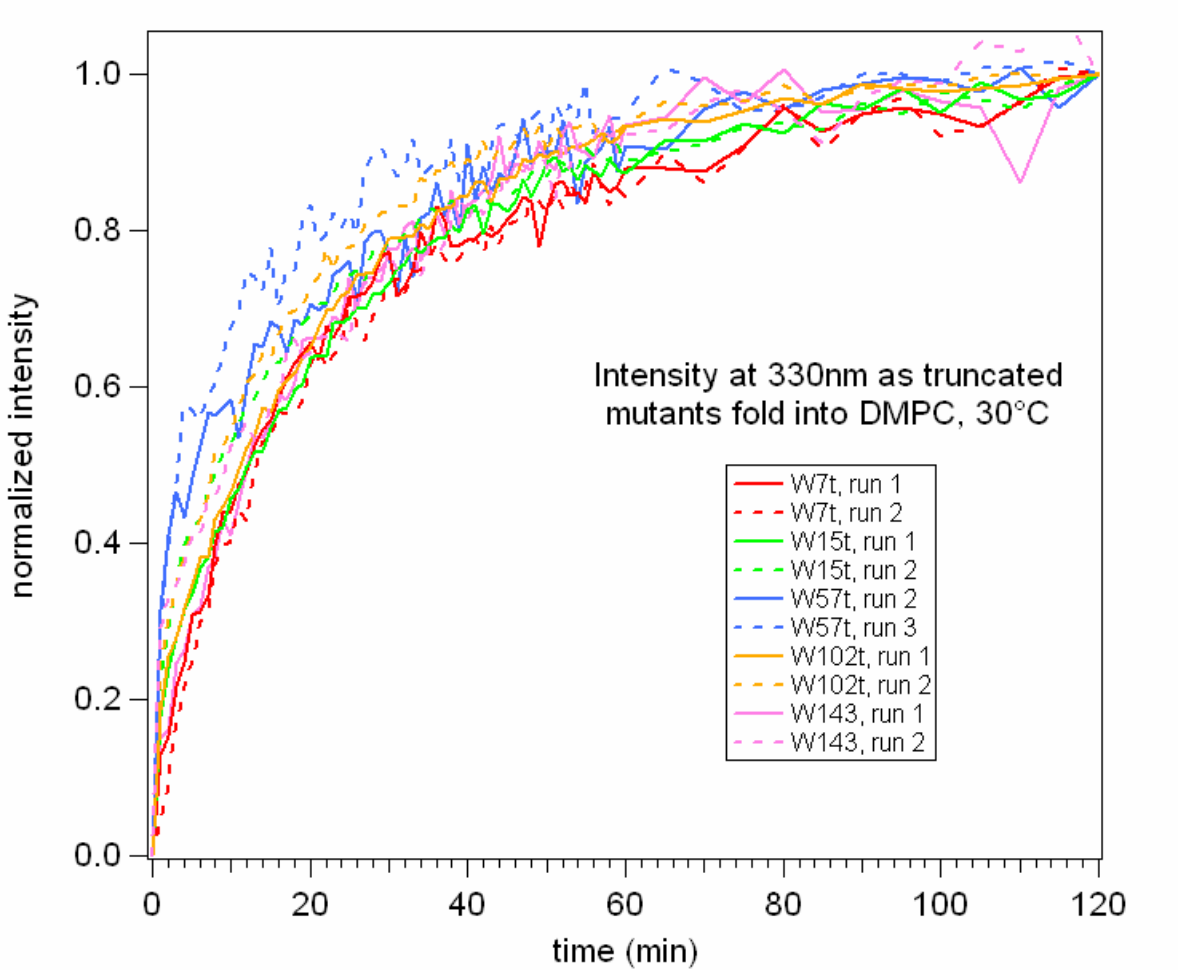


**Figure 5.12.** Fluorescence intensity of Trp mutants monitored at 330 nm immediately following initiation of folding reaction in DMPC for truncated mutants. Kinetic traces were normalized to have equivalent maximum emission intensities at 120 minutes.

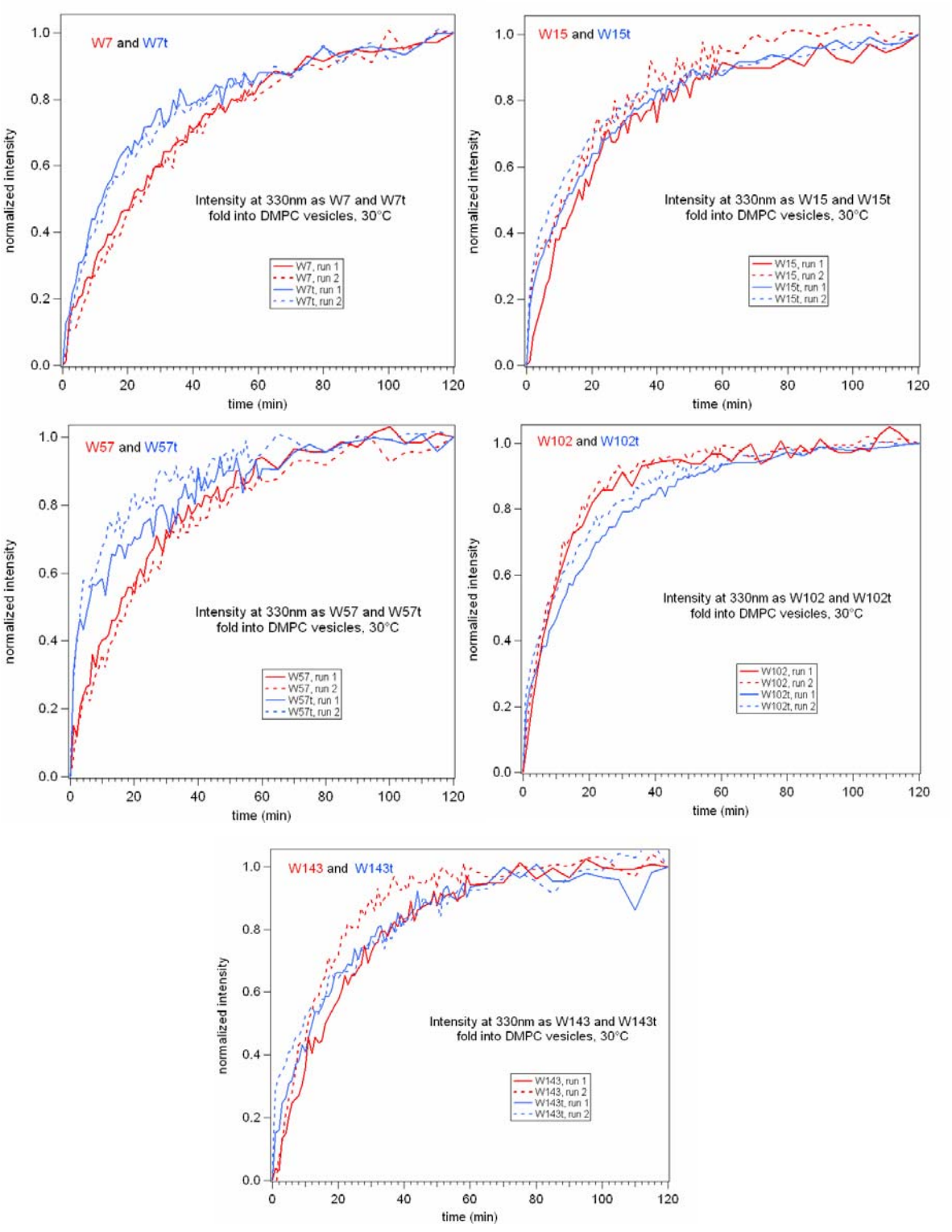


**Figure 5.13.** Overlay of fluorescence intensity at 330 nm for full-length and truncated mutants at each Trp position.

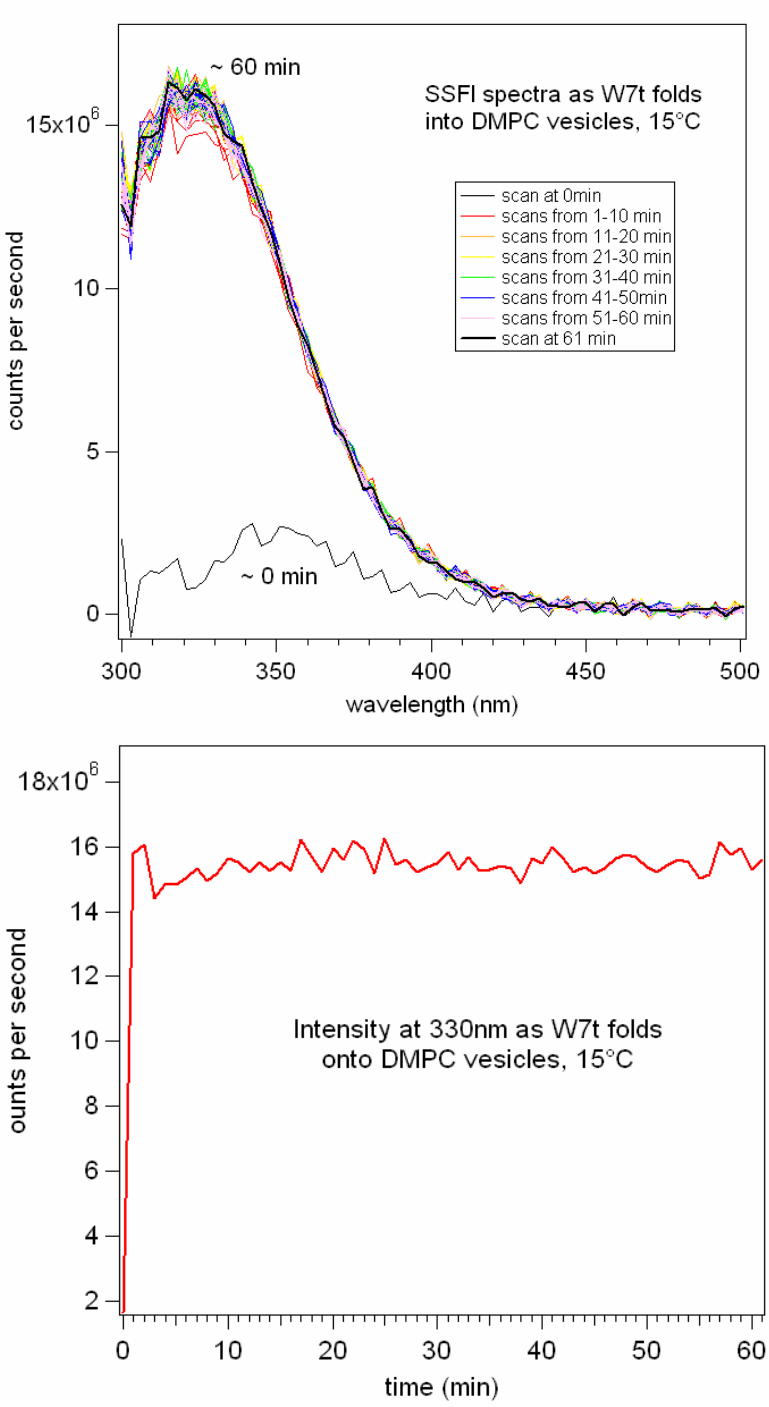


**Figure 5.14.** Fluorescence spectra (top) of W7t immediately following protein injection to initiate folding into DMPC vesicles at 15 $^{o}$C. The intensity at 330 nm is shown on the bottom. Spectra are immediately blue-shifted upon addition of protein to the cold vesicles. During the 60 minutes of data collection, no changes in the spectra and 330 nm values are observed.

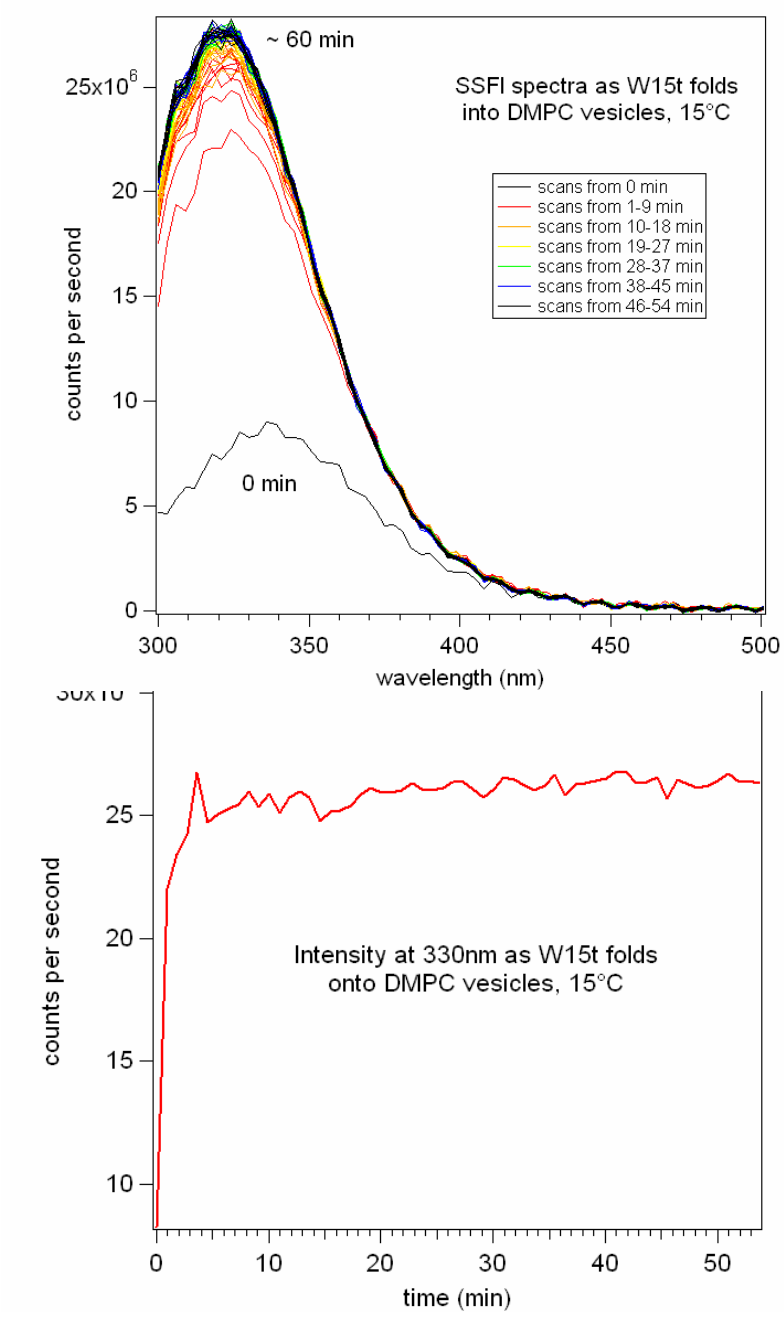


**Figure 5.15.** Fluorescence spectra (top) of W15t immediately following protein injection to initiate folding into DMPC vesicles at 15 $^{o}$C. The intensity at 330 nm is shown on the bottom. Spectra are immediately blue-shifted upon addition of protein to the cold vesicles. During the 60 minutes of data collection, no changes in the spectra and 330 nm values are observed.

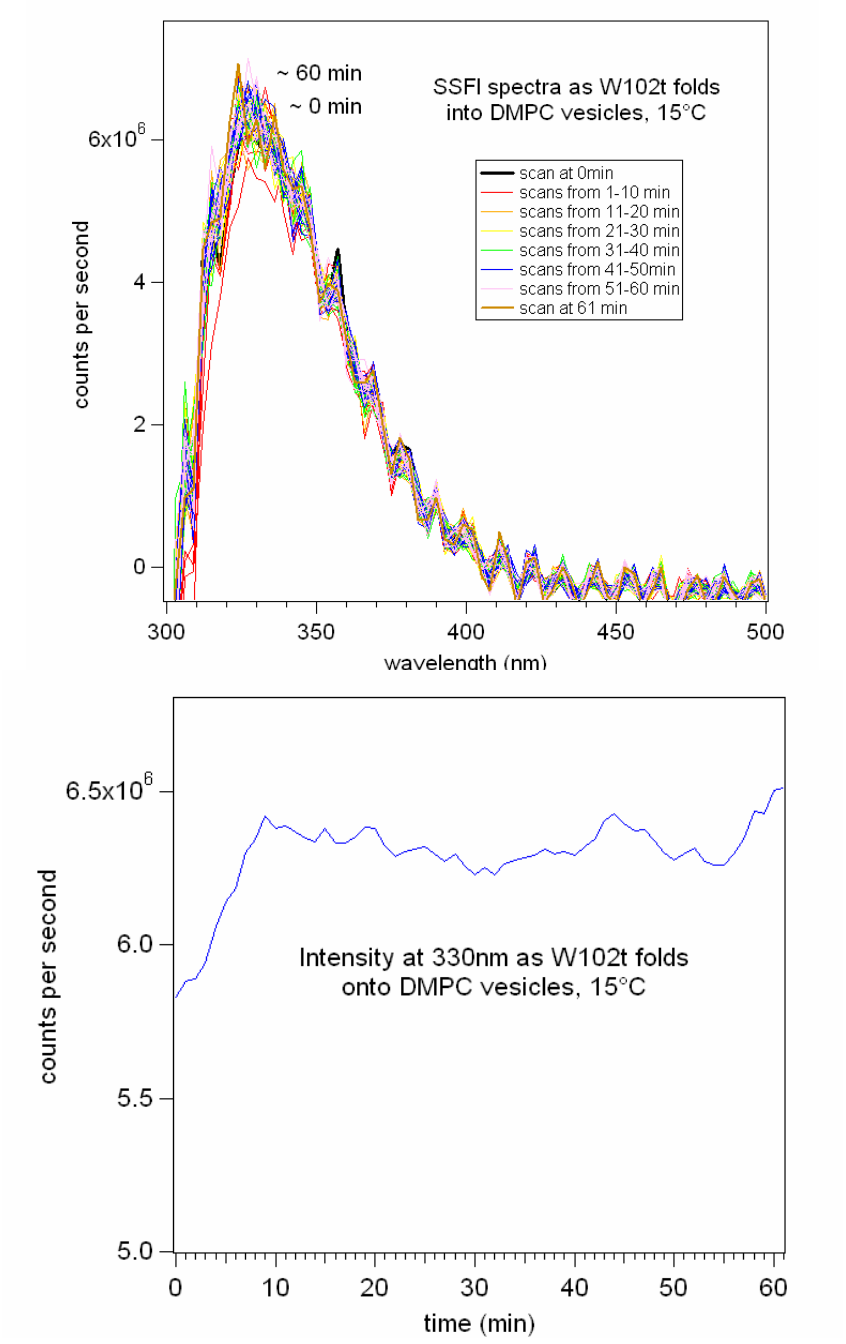


**Figure 5.16.** Fluorescence spectra (top) of W102t immediately following protein injection to initiate folding into DMPC vesicles at 15 $^{o}$C. The intensity at 330 nm is shown on the bottom. Spectra are immediately blue-shifted upon addition of protein to the cold vesicles. During the 60 minutes of data collection, very small changes in the spectra and 330 nm values are observed.

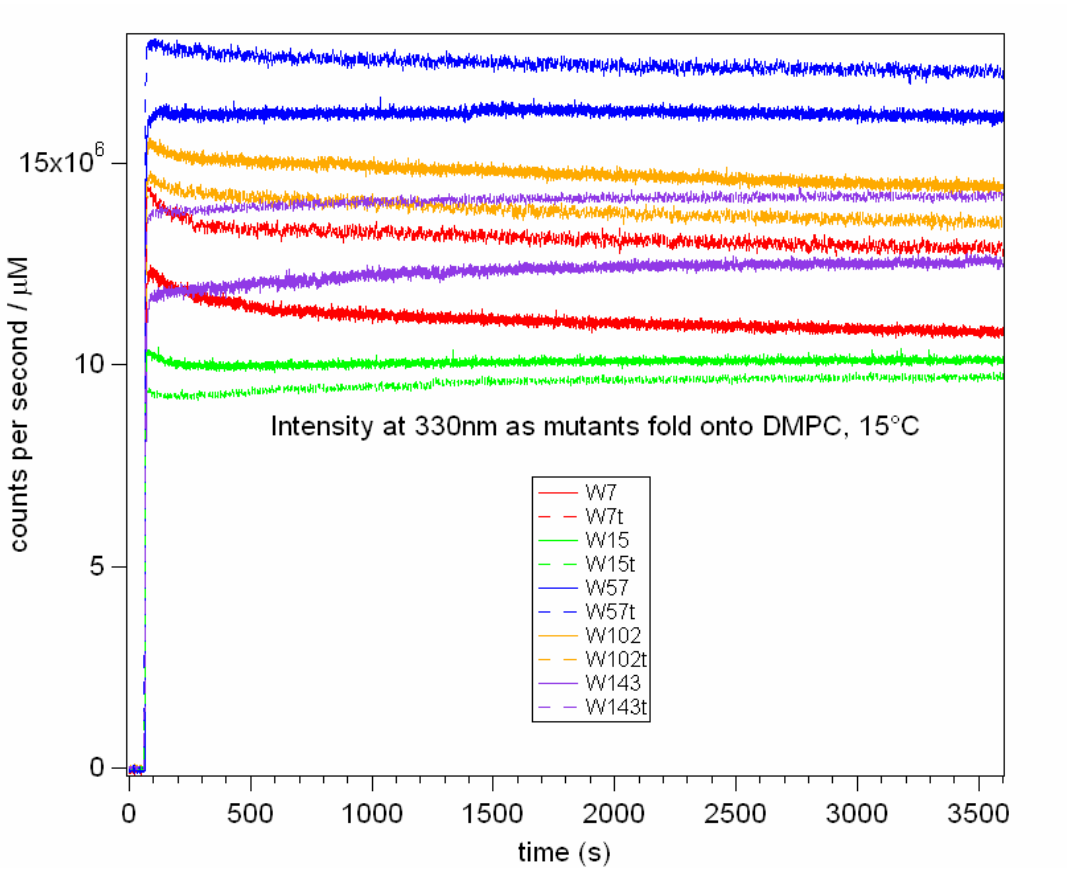


**Figure 5.17.** Fluorescence intensity measured at 330 nm for all Trp mutants immediately following protein injection to initiate adsorption onto DMPC vesicles at 15 $^{o}$C. During the 60 minutes of data collection, no changes in the 330 nm values are observed.

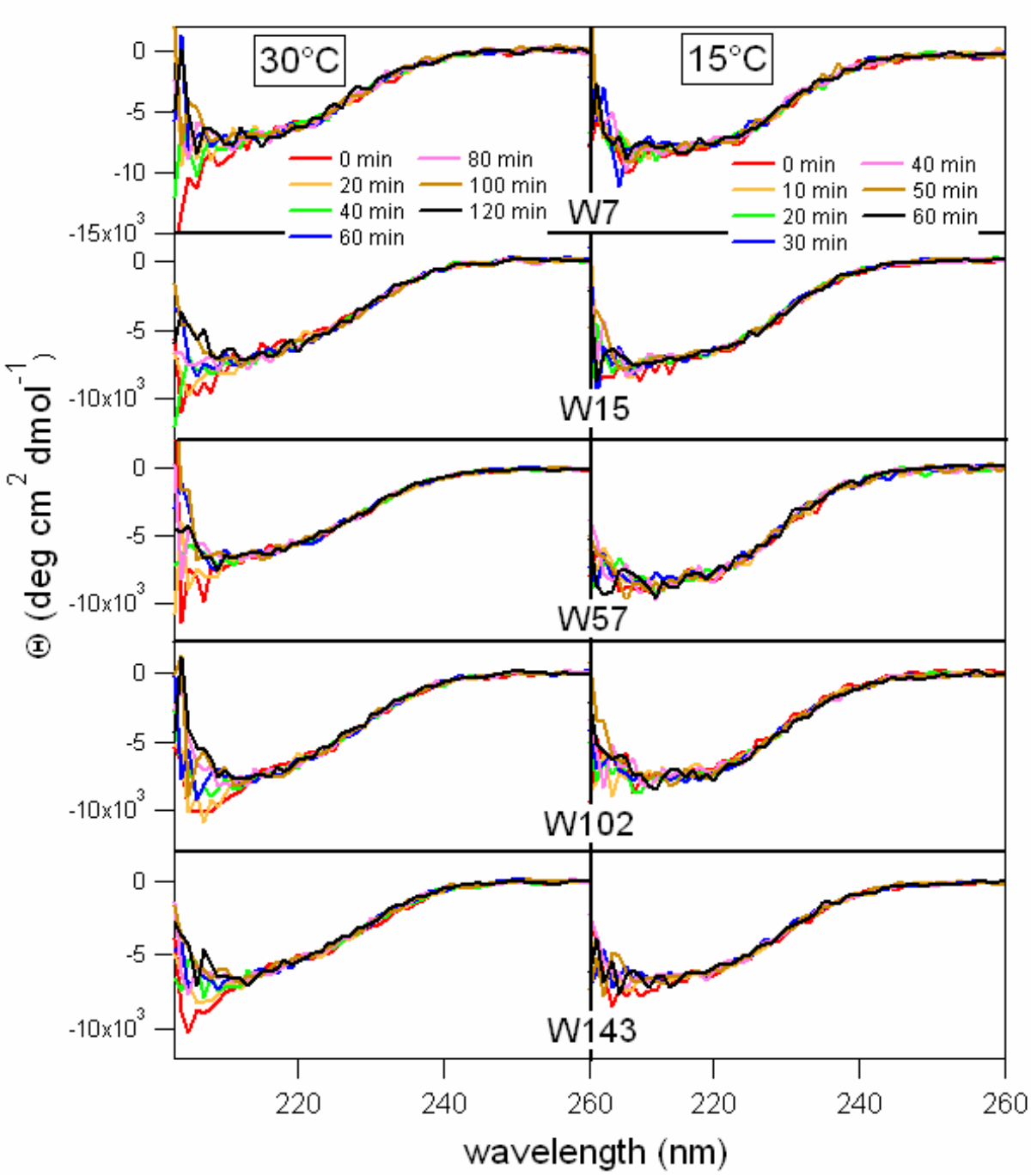


**Figure 5.18.** CD spectra of full-length Trp mutants immediately following initiation of a folding reaction in 30 °C DMPC (left) and 15 °C DMPC (right). The time scales for folding are different for 30 °C and 15 °C samples. As the protein refolds, the CD spectra evolved to form β-sheet signal for folding at 30 °C. In contrast, no changes in signal were observed for refolding at 15 °C.

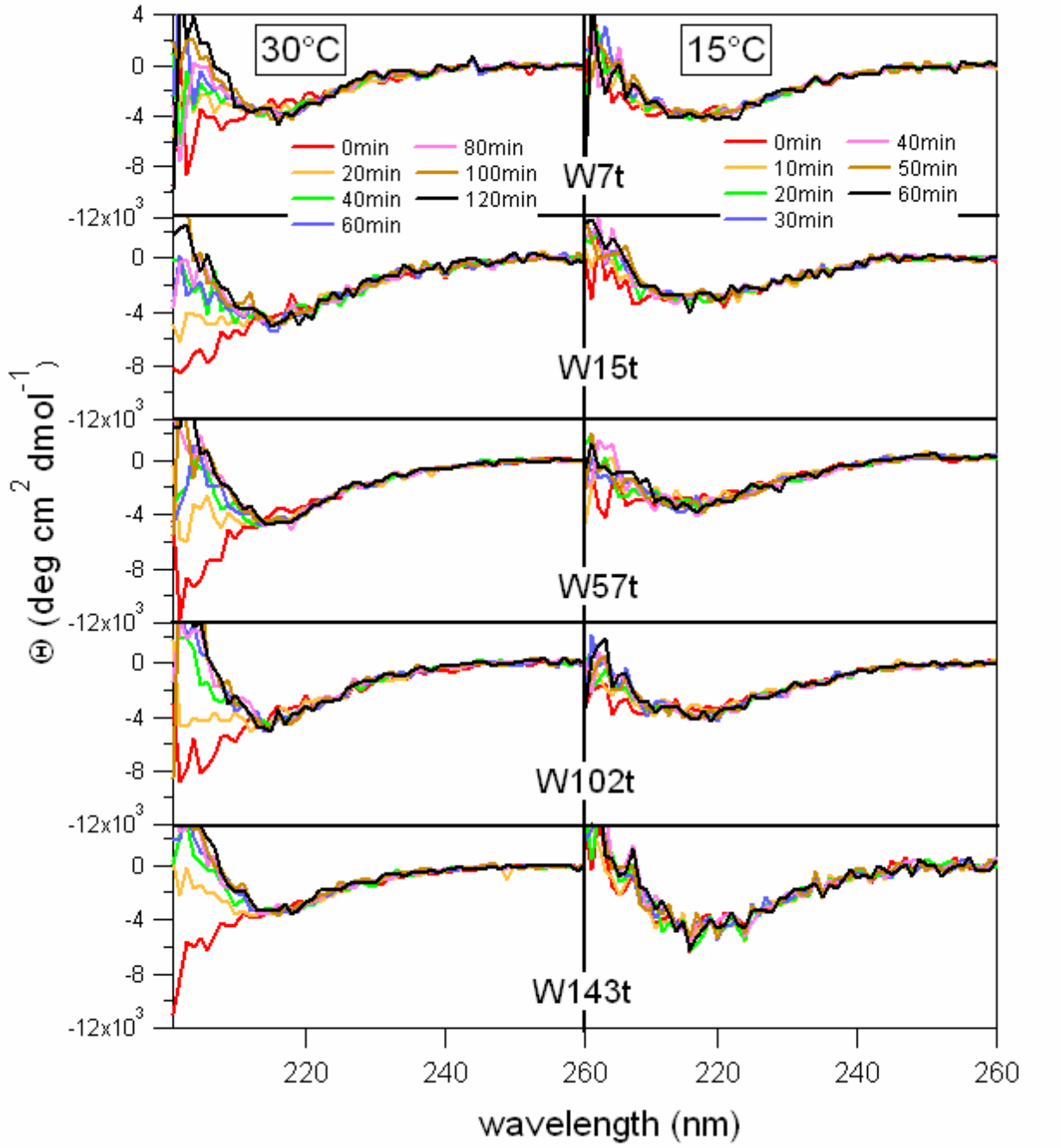


**Figure 5.19.** CD spectra of truncated Trp mutants immediately following initiation of a folding reaction in 30 °C DMPC (left) and 15 °C DMPC (right). The time scales for folding are different for 30 °C and 15 °C samples. As the protein refolds, the CD spectra evolved to form β-sheet signal for folding at 30 °C. In contrast, no changes in signal were observed for refolding at 15 °C.

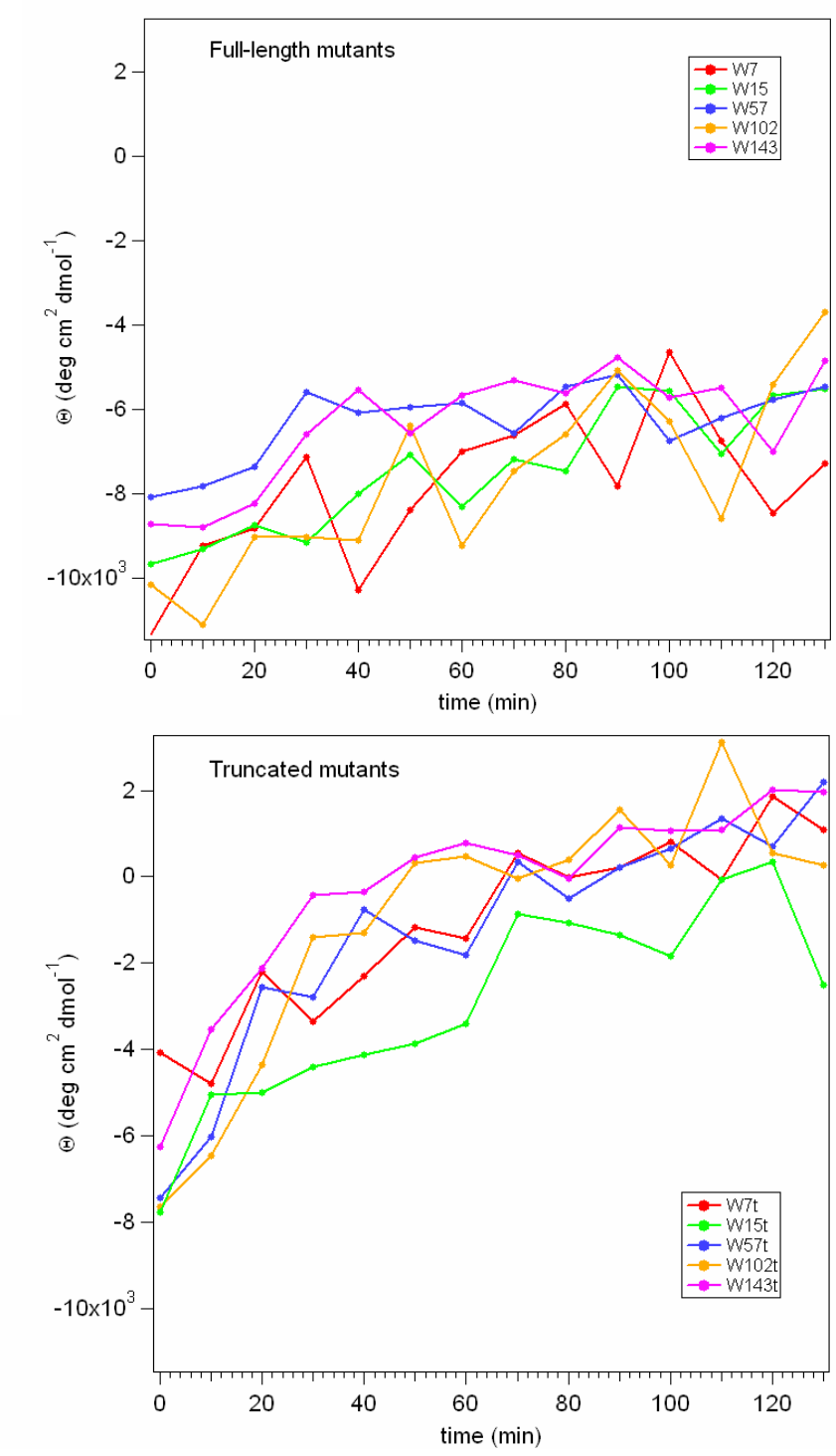


**Figure 5.20.** Top panel shows the molar ellipticity at 206 nm for full-length mutants as the proteins fold into DMPC vesicles at 30 $^{o}$C. Bottom panel shows the molar ellipticity at 206 nm for truncated mutants as the proteins fold into DMPC vesicles at 30 $^{o}$C.

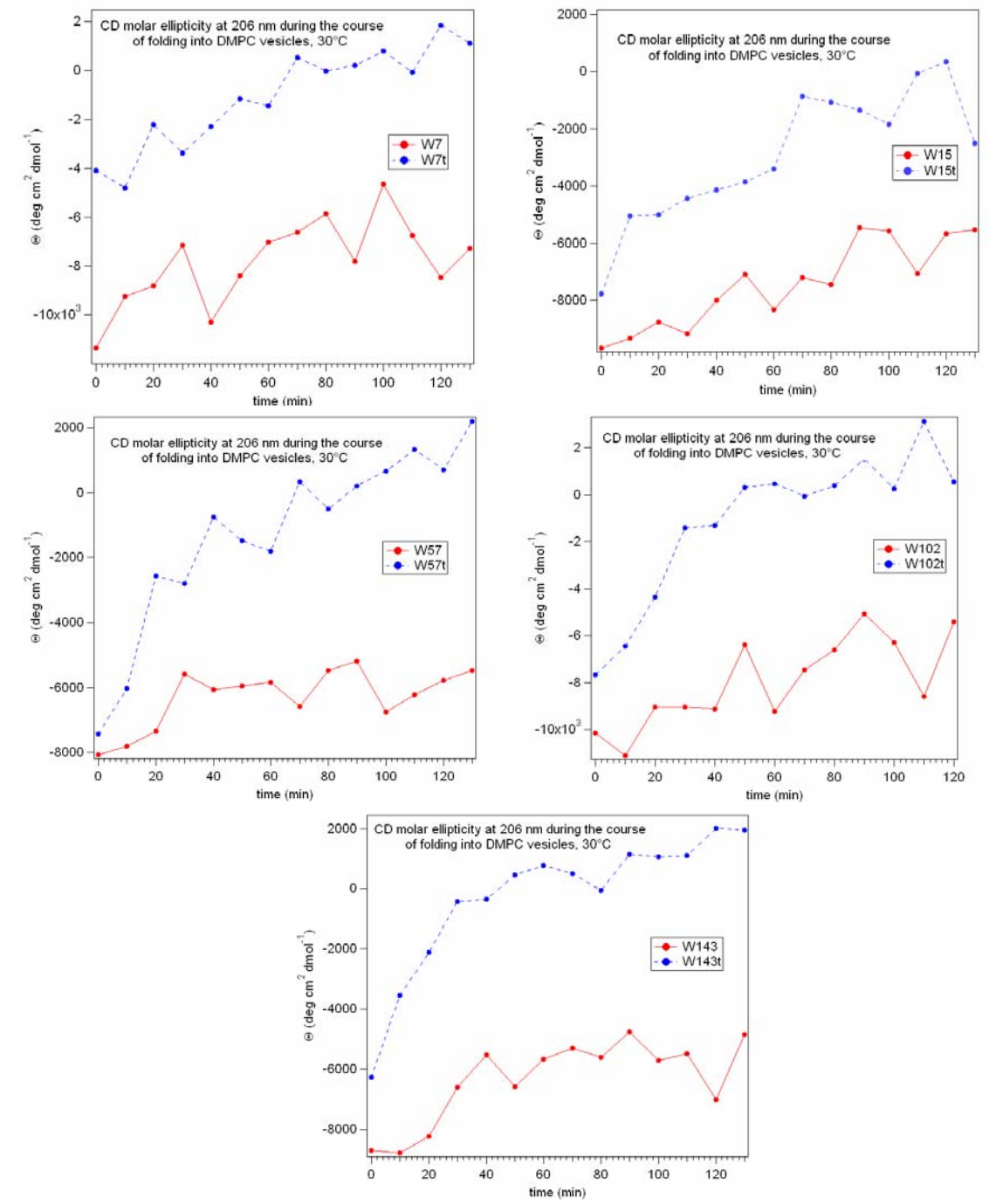


**Figure 5.21.** Changes in molar ellipticity at 206 nm for full-length mutants as the proteins fold into DMPC vesicles at 30 $^{o}$C. Blue traces are truncated mutants and red traces are full-length mutants.

## 5.5 REFERENCES


Dornmair, K., Kiefer, H., and Jahnig, F. (1990) Refolding of an integral membrane-protein - OmpA of *Escherichia-coli*, *Journal of Biological Chemistry 265*, 18907-18911.

Eisele, J. L., and Rosenbusch, J. P. (1990) *In vitro* folding and oligomerization of a membrane protein - transition of bacterial porin from random coil to native conformation, *Journal of Biological Chemistry 265*, 10217-10220.

Gudgin, E., Lopezdelgado, R., and Ware, W. R. (1983) Photophysics of tryptophan in $H_2O$, $D_2O$, and in non-aqueous solvents, *Journal of Physical Chemistry 87*, 1559-1565.

Huang, K. S., Bayley, H., Liao, M. J., London, E., and Khorana, H. G. (1981) Refolding of an integral membrane-protein - denaturation, renaturation, and reconstitution of intact bacteriorhodopsin and 2 proteolytic fragments, *Journal of Biological Chemistry 256*, 3802-3809.

Kleinschmidt, J. H., and Tamm, L. K. (1996) Folding intermediates of a beta-barrel membrane protein. Kinetic evidence for a multi-step membrane insertion mechanism, *Biochemistry 35*, 12993-13000.

Kleinschmidt, J. H., den Blaauwen, T., Driessen, A. J. M., and Tamm, L. K. (1999) Outer membrane protein A of Escherichia coli inserts and folds into lipid bilayers by a concerted mechanism, *Biochemistry 38*, 5006-5016.

Kleinschmidt, J. H., and Tamm, L. K. (1999) Time-resolved distance determination by tryptophan fluorescence quenching: Probing intermediates in membrane protein folding, *Biochemistry 38*, 4996-5005.

Kleinschmidt, J. H., and Tamm, L. K. (2002) Secondary and tertiary structure formation of the beta-barrel membrane protein OmpA is synchronized and depends on membrane thickness, *Journal of Molecular Biology 324*, 319-330.

Kleinschmidt, J. H. (2003) Membrane protein folding on the example of outer membrane protein A of Escherichia coli, *Cellular and Molecular Life Sciences 60*, 1547-1558.

Lakowicz, J. R. (1999) *Principles of fluorescence spectroscopy*, 2nd edition ed., Kluwer Academic/Plenum Publishers, New York, NY.

Paulsen, H., Rumler, U., and Rudiger, W. (1990) Reconstitution of pigment-containing complexes from light-harvesting chlorophyll - A/B binding protein overexpressed in *Escherichia-coli*, *Planta 181*, 204-211.

Rodionova, N. A., Tatulian, S. A., Surrey, T., Jahnig, F., and Tamm, L. K. (1995) Characterization of 2 membrane-bound forms of OmpA, *Biochemistry 34*, 1921-1929.

Schiffer, M., Chang, C. H., and Stevens, F. J. (1992) The functions of tryptophan residues in membrane-proteins, *Protein Engineering 5*, 213-214.

Surrey, T., and Jahnig, F. (1992) Refolding and oriented insertion of a membrane-protein into a lipid bilayer, *Proceedings of the National Academy of Sciences of the United States of America 89*, 7457-7461.

Surrey, T., and Jahnig, F. (1995) Kinetics of folding and membrane insertion of a beta-barrel membrane protein, *Journal of Biological Chemistry 270*, 28199-28203.

Surrey, T., Schmid, A., and Jahnig, F. (1996) Folding and membrane insertion of the trimeric beta-barrel protein OmpF, *Biochemistry 35*, 2283-2288.

White, S. H., and Wimley, W. C. (1999) Membrane protein folding and stability: Physical principles, *Annual Review of Biophysics and Biomolecular Structure 28*, 319-365.